

1
2 Acknowledgements

3 The final publication is available at link.springer.com:

4 <http://link.springer.com/article/10.1007/s00253-015-7020-4>

5 doi:10.1007/s00253-015-7020-4

6 The online version of this article contains supplementary material, which is available to authorized
7 users.
8
9

10
11
12
13
14
15
16
17
18
19
20 1 Journal: **Applied Microbiology and Biotechnology**

21
22 2

23
24 3

25
26 4 Manuscript title: **Increased chitin biosynthesis contributes to the**
27
28 5 **resistance of *Penicillium polonicum* against the antifungal protein**
29
30 6 **PgAFP.**

31
32 7

33
34 8 Authors: Josué Delgado,^a Rebecca A. Owens,^b Sean Doyle,^b Miguel A.
35
36 9 Asensio^a and Félix Núñez.^a

37
38
39 10

40
41 11 Affiliations and addresses:

42
43 12 ^a Food Hygiene and Safety, Institute of Meat Products, University of
44
45 13 Extremadura, Cáceres, Spain.

46
47 14 ^b Department of Biology, Maynooth University, Maynooth, Co. Kildare,
48
49 15 Ireland.

50
51
52 16

53
54 17 Corresponding author:

55
56 18 Miguel A. Asensio

57
58 19 masensio@unex.es, Tel.: +34 927 257124; Fax: +34 927 257110.

59
60 20
61
62
63
64
65

1 21 **ABSTRACT**

2
3
4 22 Antifungal proteins from molds have been proposed as a valuable tool against unwanted molds, but the
5 23 resistance of some fungi limits their use. Resistance to antimicrobial peptides has been suggested to be
6 24 due to lack of interaction with the mold or to a successful response. The antifungal protein PgAFP
7 25 produced by *Penicillium chrysogenum* inhibits the growth of various ascomycetes, but not *Penicillium*
8 26 *polonicum*. To study the basis for resistance to this antifungal protein, localization of PgAFP and
9 27 metabolic, structural, and morphological changes were investigated in *P. polonicum*. PgAFP bound the
10 28 outer layer of *P. polonicum* but not regenerated chitin, suggesting an interaction with specific molecules.
11 29 Comparative two-dimensional gel electrophoresis (2D-PAGE) and comparative quantitative proteomics
12 30 revealed changes in the relative abundance of several proteins from ribosome, spliceosome, metabolic,
13 31 and biosynthesis of secondary metabolite pathways. The proteome changes and an altered permeability
14 32 reveal an active reaction of *P. polonicum* to PgAFP. The successful response of the resistant mold seems
15 33 to be based on the higher abundance of protein Rho GTPase Rho1 that would lead to the increased chitin
16 34 deposition via cell wall integrity (CWI) signaling pathway. Thus, combined treatment with chitinases
17 35 could provide a complementary means to combat resistance to antifungal proteins.

18
19
20
21
22
23
24
25
26 36 **KEYWORDS**

27
28
29 37 Antifungal proteins, proteomics, resistance, *Penicillium polonicum*, chitin, cell-wall integrity pathway

30
31
32 38 **INTRODUCTION**

33
34 39 The antifungal protein PgAFP produced by the strain *Penicillium chrysogenum* CECT 20922 (formerly
35 40 RP42C) is within a group of small, highly basic and low molecular mass proteins (Rodríguez-Martín et al.
36 41 2010). PgAFP inhibits various pathogenic and spoilage ascomycetes of interest in foods, including strains
37 42 of various *Aspergillus* spp., such as *A. carbonarius*, *A. flavus*, *A. ochraceus*, *A. fumigatus*, and *A.*
38 43 *tubingensis*, as well as *Penicillium* spp., such as *P. commune*, *P. restrictum*, *P. nalgiovense*, and *P.*
39 44 *chrysogenum* (Delgado et al. 2015a). However, *Penicillium polonicum* and the PgAFP-producer strain of
40 45 *P. chrysogenum* were not inhibited by PgAFP.

41 46 Other antifungal proteins produced by ascomycetes are PAF from *P. chrysogenum* Q176 (Marx et al.
42 47 1995), Pc-Arctin from *P. chrysogenum* A096 (Chen et al. 2013), BP from *Penicillium brevicompactum*
43 48 (Seibold et al. 2011) AFP and AFP_{NN5353} from *Aspergillus giganteus* (Nakaya et al. 1990; Binder et al.
44 49 2011), Anafp from *Aspergillus niger* (Gun Lee et al. 1999), AcAFP and AcAMP from *Aspergillus*
45 50 *clavatus* (Skouri-Gargouri and Gargouri 2008; Hajji et al. 2010), FPAP from *Fusarium polyphialidicum*
46 51 (Galgóczy et al. 2013b) and NFAP from *Neosartorya fischeri* (Kovács et al. 2011). Mechanisms of action
47 52 of antifungal proteins from molds have been described as multifactorial, where membrane
48 53 permeabilization, changes in actin distribution, chitin biosynthesis inhibition, destabilization of cell wall,
49 54 and oxidative stress lead to apoptosis (Leiter et al. 2005; Moreno et al. 2006; Hagen et al. 2007; Binder et
50 55 al. 2010; Virágh et al. 2015; Delgado et al. 2015b). AFP binds chitin, inhibits chitin biosynthesis,
51 56 permeabilizes the cell membrane, and penetrates into the cell and binds nucleic acids (Liu et al. 2002;

57 Moreno et al. 2006; Hagen et al. 2007) and AcAFP also binds chitin altering cell wall (Skouri-Gargouri et
58 al. 2009), whereas PAF, NFAP, and PgAFP lead to apoptosis mediated by G-protein signaling (Binder et
59 al. 2010; Binder et al. 2015; Virágh et al. 2015; Delgado et al. 2015b). Both PAF and NFAP activate the
60 cAMP/Protein kinase A pathway via G-protein signaling (Leiter et al. 2005; Virágh et al. 2015) and
61 PgAFP provoked a lower amount G-protein subunit β CpcB (Delgado et al. 2015b).
62 However, the defensive strategies of resistant molds are poorly described. The lack of electrostatic
63 affinity or receptors in cell surfaces has been suggested as the cause of the resistance to antimicrobial
64 peptides (Yeaman and Yount 2003). PgAFP does not bind to the producer strain *P. chrysogenum* CECT
65 20922 that withstands at least 312 μ g/ml (Delgado et al. 2015a, b). The lack of interaction between
66 antifungal proteins and mold surface results in the absence of major metabolic responses in the resistant
67 fungi. Another successful strategy of resistant fungi to counteract AFP is chitin synthesis stimulation
68 (Ouedraogo et al. 2011). The latter strategy implies interaction with the resistant fungus and active
69 metabolic response to the antifungal protein. Thus, studying the mechanisms involved in the resistance
70 requires in depth investigation of the metabolic response of resistant fungi to antifungal proteins.
71 Comparative proteomic analysis is a powerful tool to study metabolic changes at the molecular level
72 (Kim et al. 2007). 2D-PAGE has the ability to separate complete proteins including those with post-
73 translational modifications, but only a small percentage of the whole proteome is revealed (Görg et al.
74 2009). On the other hand, comparative quantitative proteomics is able to identify proteins not detectable
75 by 2D-PAGE. These two techniques have been used to complementarily evaluate the effect of PgAFP on
76 the proteins involved in signaling pathways and selecting adequate tests to study the metabolic response
77 in molds (Delgado et al. 2015b). In addition, localization of the antifungal protein in non-sensitive molds
78 can give valuable information on the possible interaction at the surface or inside the cell. Given that
79 antifungal proteins provoke oxidative stress leading to apoptosis in sensitive mold, knowing the extent of
80 these two phenomena in resistant molds would contribute to clarify the defence mechanism.
81 To study the effect of PgAFP on resistant molds, *P. polonicum* was chosen because it was the only
82 resistant ascomycete known, apart from the PgAFP-producer *P. chrysogenum* CECT 20922 (Delgado et
83 al. 2015a). *A. niger* has been used as sensitive control with various antifungal proteins (Kaiserer et al.
84 2003; Hagen et al. 2007; Kovács et al. 2011). *A. tubingensis* CECT 20932, formerly *A. niger* An261, has
85 been used in the present work as sensitive control because it is the closest species to *A. niger* known to be
86 sensitive to PgAFP (Delgado et al. 2015a).
87 The aim of this work was to investigate the effect of PgAFP on the proteome profile and selected
88 characteristics to disclose the resistance response of *P. polonicum*. Localization of PgAFP was studied for
89 a better understanding of the interaction with *P. polonicum*. This knowledge would allow designing new
90 strategies to maximize the inhibition effect and spectra of PgAFP in molds.

91 MATERIAL AND METHODS

92 **Strains**

93 In vitro tests were carried out with three molds isolated from dry-cured ham available from the Spanish
94 Type Culture Collection (CECT, Valencia, Spain): *P. chrysogenum* CECT 20922, *P. polonicum* CECT
95 20933 and *A. tubingensis* CECT 20932.

96 **Purification of PgAFP**

97 PgAFP was obtained from *P. chrysogenum* CECT 20922 grown in potato dextrose broth (PDB, Scharlab,
98 Barcelona, Spain) pH 4.5, at 25 °C for 21 days, as described previously (Acosta et al. 2009). To get cell-
99 free medium, mycelium was removed by filtering through Miracloth (Calbiochem, Darmstadt, Germany)
100 and the culture medium was filtered through a nitrocellulose 0.22 µm-pore-size (Sartorius, Goettingen,
101 Germany). Cell-free media were applied to an ÄKTA FPLC with a cationic exchange column HiTrap SP
102 HP (Amersham Biosciences, Uppsala, Sweden) with 20 mM sodium acetate, pH 4.5. Adsorbed proteins
103 were eluted with 20 mM sodium acetate buffer (pH 4.5) containing 1 M NaCl and detected at 214 nm.
104 The fraction containing PgAFP protein was then gel filtered on a HiLoad 26/60 Superdex 75 column for
105 FPLC (Amersham Biosciences, Uppsala, Sweden) using 50 mM sodium phosphate buffer, pH 7
106 containing 0.15 M NaCl as elution buffer. PgAFP concentration in a pooled stock solution was measured
107 by Lowry method (Lowry et al. 1951), sterilised through 0.22 µm acetate cellulose filters (Fisher
108 Scientific) and stored at -20 °C until use.

109 **Effect of PgAFP on mold growth**

110 As a preliminary test, to confirm the known effect of PgAFP on growth of both sensitive and resistant
111 molds in malt extract broth (Delgado et al. 2015a), *P. polonicum* and *A. tubingensis* were grown in PDB
112 treated with PgAFP in the whole range of concentrations used in this work (0 to 75 µg/ml) for 96 h.

113 **Proteomics**

114 To obtain the protein extracts, *P. polonicum* CECT 20933 was cultured in triplicate in 50 ml of PDB, at
115 25 °C with continuous shaking at 200 rpm in either presence (10µg/ml) or absence of PgAFP. Mycelia
116 were harvested, filtered, washed, and lysed as previously described (Carberry et al. 2006). Mycelial
117 lysates were centrifuged to remove cell debris and the subsequent supernatant precipitated with
118 TCA/acetone (Carpentier et al. 2005). The following two proteomic analysis were carried out from these
119 precipitated lysates, similar to the procedure described by Delgado et al. (2015b).

120 **Two-dimensional electrophoresis.** For protein separation by 2D-PAGE, resuspended extracts containing
121 250 µg of protein were loaded onto Immobiline Dry strips (IPG strip; Amersham Biosciences) in the pH
122 range 4–7, followed by electrofocusing, and electrophoresis as described previously (Carberry et al.
123 2006). Gels obtained from 3 biological replicates and 2 technical replicates per treatment were stained
124 and analyzed using Progenesis™ SameSpot software (TotalLab, Newcastle, UK) as previously described
125 (O’Keeffe et al. 2013; Collins et al. 2013; Owens et al. 2014). Spot intensities were normalised in
126 Progenesis SameSpots software (Delgado et al. 2015b). Protein spots showing differences ($p < 0.05$, fold
127 change ≥ 1.5) were excised, destained, in-gel trypsin-digested (Shevchenko et al. 2007). Then, samples
128 were sonicated and the digested supernatant was dried, resuspended in 0.1% formic acid, and filtered
129 through 0.22 µm cellulose spin-filters according to Delgado et al. (2015b).

130 The samples were loaded onto a Zorbax 300 SB C-18 Nano-HPLC Chip and analysed by a 6340 Model
131 Ion Trap LC-Mass Spectrometer (Agilent Technologies, Dublin, Ireland) using electrospray ionisation.
132 The eluted peptides were ionized and analysed by mass spectrometry. MSⁿ analysis was carried out on the
133 three most abundant peptide precursor ions at each time point, as selected automatically by the mass
134 spectrometer. MASCOT MS/MS Ion search, NCBI (National Centre for Biotechnology Information,
135 www.ncbi.nlm.nih.gov/guide/proteins/) database and KEGG (Kioto Encyclopedia of Genes and Genome,
136 www.genome.jp/kegg/) were used for protein identification and function, also BLAST® protein was
137 employed to find orthologous proteins.

138 **Label-free proteomics.** Proteins precipitated from three biological replicates were resuspended in 8 M
139 urea, dithiothreitol reduced and iodoacetic acid alkylated (Collins et al. 2013), and trypsin digested.
140 Digested samples were desalted using C18 ZipTips® (Millipore, Darmstadt, Germany). One microgram
141 from each digest was analysed via a Thermo Scientific Q-Exactive mass spectrometer coupled to a
142 Dionex RSLCnano (Thermo Scientific, Waltham, MA, USA). Data was collected using a Top15 method
143 for MS/MS scans (Dolan et al. 2014; O’Keeffe et al. 2014). Comparative proteome abundance and data
144 analysis was performed using MaxQuant software (Version 1.3.0.5; www.maxquant.org/downloads.htm)
145 (Cox and Mann 2008), with Andromeda used for database searching and Perseus (Version 1.4.1.3) used
146 to organise the data, as per Delgado et al. (2015b). Data were searched against a *P. chrysogenum* database
147 from Uniprot (www.uniprot.org; March 2014). In the absence of sequenced *P. polonicum* or any other
148 species from Section *Fasciculata* (Houbraken and Samson 2011), *P. chrysogenum* also from subgenus
149 *Penicillium*, was chosen for comparison. Quantitative analysis was performed using a t-test. Due to the
150 high sensitivity and larger dynamic range of the gel-free proteomics analyses only proteins with a *p* value
151 < 0.05 and fold change ≥ 2 were included in the quantitative results (Dolan et al. 2014; O’Keeffe et al.
152 2014). Qualitative analysis was also performed, to detect proteins that were found in at least 2 replicates
153 of a particular sample, but undetectable in the comparison sample. Blast2GO analysis was utilized to
154 further elucidate putative functions of proteins identified with abundance changes (Conesa et al. 2005).

155 **Hyphal morphology**

156 *P. polonicum* and *A. tubingensis* were grown on tubes containing 300 µl of PDB at 25 °C for 24 h in
157 either the presence (75 µg/ml) or absence of PgAFP. Mycelia were collected by centrifugation and
158 observed on a microscope Eclipse E200 equipped with a digital camera DS-Fi2 (Nikon, Tokyo, Japan).

159 **Metabolic tests**

160 To study the response to PgAFP, various metabolic tests were performed as described previously
161 (Delgado et al. 2015b). For this, the resistant *P. polonicum* (c.a. 5 x 10⁵ conidia per ml) was cultured in
162 PDB at 25 °C for 24 h in static conditions with and without PgAFP. To rule out even potential weak
163 effects, the highest concentration of 75 µg/ml PgAFP was used. Additionally, to study the effect on
164 membrane permeability throughout a wide concentration range of PgAFP (i.e. 75, 37.5, 18.75, 9.38, 4.69,
165 2.34, 1.17, and 0 µg/ml) were assayed.

166 To test membrane permeability, cultures in microtiter plates were supplemented with SYTOX Green
167 (Molecular Probes, Eugene, OR, USA) at final concentration of 0.2 µM. The fluorescence emitted was
168 measured at 10, 30, and 210 min.

169 Metabolic activity was assessed by FUN-1 staining. Grown mycelia was washed with 10 mM HEPES
170 (pH 7.5) before staining with 100 µl FUN-1 (Molecular Probes, Eugene, OR, USA) for 30 min at 25 °C
171 as described previously (Kaiserer et al. 2003). Stained hyphae were visualized and photographed by
172 fluorescence microscopy. Induction of reactive oxygen species (ROS) production was evaluated using 20
173 µM 2', 7' dichlorofluorescein diacetate (Molecular Probes, Eugene, OR, USA) according to Kaiserer et
174 al. (2003), and observed by fluorescence microscopy.
175 Membrane integrity was assessed by the acridine orange/ethidium bromide (AO/EB) double staining.
176 Hyphae were stained with 4 µg/ml of AO/EB (Sigma-Aldrich, St. Louis, MO, USA), incubated for 30
177 min, washed, and observed by fluorescence microscopy.
178 To distinguish between necrotic, late apoptotic, and viable cells, the Apoptosis Detection Kit (Sigma-
179 Aldrich, St. Louis, MO, USA), composed by Annexin V-fluorescein isothiocyanate/propidium iodide
180 (AnV-FITC/PI), was used according to manufacturer's instructions.
181 For each of these metabolic tests, the sensitive *A. tubingensis* was used as a positive control to confirm
182 the effect of PgAFP in the various assays.

183 **Chitin staining**

184 Conidia of *P. polonicum* were inoculated on 10 ml PDB in Petri dish containing a coverglass and
185 incubated in presence (75µg/ml) and absence of PgAFP at 25 °C for 24 h. Mycelium was fixed, stained
186 for 5 min with fluorescent brightener 28 (Sigma-Aldrich, St. Louis, MO, USA), and then washed, to
187 visualize chitin (Harris et al. 1994) in a fluorescence microscope with an excitation wavelength of 387/11
188 nm.

189 **Effect of PgAFP combined with chitinase on *P. polonicum* growth**

190 Four different batches were prepared by pouring the reagents onto 15 ml potato dextrose agar plates made
191 with PDB (Scharlab, Barcelona, Spain) and 20 g/l bacteriological agar (Scharlab, Barcelona), as follows:
192 a) 2.5 ml of 600 µg/ml PgAFP in phosphate elution buffer and 0.1 ml PBS, b) 2.5 ml of phosphate elution
193 buffer and 0.1 ml of ≥ 60 units/ml chitinase from *Streptomyces griseus* (Sigma-Aldrich, St. Louis, MO,
194 USA) in PBS, c) and 2.5 ml of 600 µg/ml PgAFP in phosphate elution buffer and 0.1 ml of ≥ 60 units/ml
195 chitinase from *S. griseus* (Sigma-Aldrich, St. Louis, MO, USA) in PBS, and d) 2.5 ml of phosphate
196 elution buffer and 0.1 ml PBS as a control samples. Every plate was surface three-point inoculated with
197 10 µl of a suspension containing 10⁴ conidia and incubated at 25 °C for 168 h. The diameter of the
198 colonies were measured every 24 h. To elucidate whether the combined treatment of PgAFP and chitinase
199 has an additive or synergistic effect, the expected efficacy of this combination was determined by the
200 Abbott formula and the interaction ratio as described by Moreno et al. (2003). Interaction ratios between
201 0.5 and 1.5 are considered to be additive interactions and ratios over 1.5 are considered to be synergistic
202 interactions.

203 **Chitin binding ability of PgAFP**

204 Regenerated chitin was prepared as previously described (Souza et al. 2009), using chitin powder from
205 crab shells (Sigma-Aldrich, St. Louis, MO, USA) added to concentrated HCl with vigorous stirring,
206 filtered, and precipitated with ethanol 95%. The precipitate was filtered and washed with water until

207 neutral pH. Chitin-PgAFP binding assay was carried out as described Liu et al. (2002). Briefly, three
208 different amounts of PgAFP were mixed with 4 mg of regenerated chitin in a 0.5 ml 0.1 M Tris-HCl pH
209 7.4, 0.15 M NaCl buffer, incubated in ice for 1 h with stirring every 15 min. After incubation, samples
210 were centrifuged and the quantity of protein contained in the supernatant was measured by the method
211 described by Lowry (Lowry et al. 1951).

212 **PgAFP localization**

213 PgAFP was labelled by DareBio S.L. (Elche, Spain) as described previously (Delgado et al. 2015b). For
214 this, 100 µl of 20 mM fluorescein isothiocyanate (FITC; Anaspec, Fremont, CA, USA) in
215 dimethylsulphoxide was added to 4 ml of PgAFP (369 µg/ml), and left for 8 h at room temperature in the
216 dark. Then, 100 µl of 0.8 M Tris-HCl pH 8 were added and dialyzed against PBS.

217 *P. polonicum* and *A. tubingensis* were grown in PDB in presence of 20 µg/ml PgAFP-FITC for 24 h at 25
218 °C. Hyphae were washed twice with PBS and visualized by fluorescence microscopy with excitation
219 wavelength of 482/35 nm.

220 **Statistical analysis**

221 Statistical analyses were performed with the IBM SPSS v.22 (www-
222 03.ibm.com/software/products/es/spss-stats-standard). Growth inhibition and membrane permeability data
223 were tested for normality (Kolmogorov-Smirnov with Lilliefors correction) and homoscedasticity
224 (Levene's test). Given that these data were non-normally distributed, mean values were compared using
225 nonparametric Kruskal–Wallis test. To compare treatments in pairs, Mann-Whitney *U* test was applied (*p*
226 < 0.05).

227 **RESULTS**

228 As expected, PgAFP showed no effect (*p* > 0.05) on *P. polonicum* grown in PDB in the whole range of
229 concentrations tested. *A. tubingensis* growth was affected (*p* < 0.05) from 4.7 µg/ml PgAFP at 48 h (data
230 not shown).

231 **Effect on proteome**

232 2D-PAGE comparative proteomic analysis, in presence or absence of 10 µg/ml of PgAFP, showed 37
233 spots with differences (*p* < 0.05) over 1.5 fold change in relative abundance between treated and untreated
234 *P. polonicum*. The abundance in treated samples was higher (1.5-3 fold) in 9 spots and lower (1.5-4.1
235 fold) in the remaining 27 proteins, including 2 spots from separate isoforms (Table S1 in the
236 Supplementary Material).

237 Comparative label-free quantitative proteomic analysis showed a total of 918 proteins from *P. polonicum*,
238 93 of them displayed altered relative abundance (*p* < 0.05) over two-fold change with PgAFP treatment
239 (Table S2 in the Supplementary Material). Thirty eight proteins were found in higher amounts (2-12.4
240 fold) in treated samples, 19 were only detected in treated samples, 25 were obtained in lower amounts (2-
241 663 fold) following treatment, and 11 were only detected in non-treated samples (Table S2 in the
242 Supplementary Material).

243 Eight of the nine proteins found in higher amounts in treated samples by 2D-PAGE were also detected by
244 label-free proteomic analyses, with six of them showing similar increases in both methods (Tables S1 and
245 S2 in the Supplementary Material). Also 26 of the 27 proteins found in lower relative abundance in
246 treated *P. polonicum* by 2D-PAGE were also detected by label-free proteomics. However, only 16 of
247 them were also detected at a lower relative abundance in the latter.

248 According to KEGG pathway analysis, most of the 57 proteins from label-free proteomics with higher
249 relative abundance or only detected in treated *P. polonicum* were ribosomal and spliceosomal proteins
250 (39%), or involved in biosynthesis of secondary metabolites and metabolic pathways (14%), such as
251 pyruvate decarboxylase, pyrimidine biosynthesis, glycerol kinase, and asparagine synthetase (Table 1).
252 The remaining proteins with higher relative abundance or only detected in treated samples were
253 distributed across various pathways, such as Rho GTPase Rho1 involved in MAPK signaling pathway
254 and, interestingly, glucosamine-6-phosphate N-acetyltransferase involved in chitin biosynthesis.
255 Additionally, the antifungal protein PgAFP was detected in each of the triplicate treated sample, but not
256 in any non-treated sample. Most of the proteins found in lower quantity or only detected in non-treated
257 samples were related to biosynthesis of secondary metabolites and metabolic pathways (33%), including
258 phosphoglucomutase, and glucose 6-phosphate isomerase related to glycolysis and gluconeogenesis
259 (Table 1). Only limited changes in stress-related proteins, including glyceraldehyde-3-phosphate
260 dehydrogenase (GAPDH) and heat shock proteins, were found in treated *P. polonicum* (Table S1 and S2
261 in the Supplementary Material).

262 **SYTOX Green uptake**

263 Upon PgAFP exposure up to 4.7 µg/ml, a 7 (± 3.4) % increase (± standard error) in fluorescence was
264 observed in *P. polonicum* ($p < 0.05$) at 210 min after SYTOX Green addition (Fig. 1). Fluorescence at
265 intermediate PgAFP concentrations (9.37-18.75 µg/ml) did not differ from untreated control ($p > 0.05$),
266 whilst concentrations higher than 18.75 µg/ml decreased ($p < 0.05$) permeability below the levels of
267 untreated samples, being the fluorescence values up to 21 (± 7.1) % lower at 210 min after SYTOX Green
268 addition. On the other hand, the sensitive *A. tubingensis* showed a high increase of permeability ($p <$
269 0.05) at all PgAFP concentrations assayed (Fig. 1), reaching with 9.37-18.75 µg/ml over 110 ± (9.8-15) %
270 fluorescence higher than in the untreated control.

271 **Hyphal morphology and FUN-1 staining**

272 PgAFP exposure provoked no morphological change on either *P. polonicum* or the sensitive *A.*
273 *tubingensis* (data not shown). To know whether PgAFP affects the metabolic activity, the viability was
274 evaluated with FUN-1 using *A. tubingensis* as sensitive control. The FUN-1 metabolic staining showed
275 red intravacuolar stains in both treated and untreated *P. polonicum* revealing no reduction in the
276 metabolic activity (Fig. 2). Conversely, intravacuolar red stains were not observed in PgAFP-treated *A.*
277 *tubingensis*, revealing a lower metabolic activity.

278 **Chitin staining**

279 To study the effect of PgAFP on chitin deposition on the resistant mold, the quantity of chitin was
280 estimated by staining with fluorescent brightener 28. The observed fluorescence indicated a higher chitin
281 deposition in the cell wall of treated than in non-treated *P. polonicum* (Fig. 3).

282 **Effect of PgAFP-chitinase combined treatment on *P. polonicum* growth**

283 For the whole incubation time, no statistically significant difference was found among growth of the
284 untreated control and *P. polonicum* treated only with PgAFP (Fig 4). Chitinase treatment reduced growth
285 compared to control batch. Growth of *P. polonicum* treated with combined PgAFP and chitinase was the
286 lowest ($p < 0.05$). The interaction ratios between these antifungal compounds at 96 and 120 h incubation
287 were 1.93 and 1.70, respectively. Thus, the slower growth in the combined treatment is attributed to a
288 synergistic effect of chitinase and PgAFP.

289 **PgAFP localization**

290 PgAFP localization was investigated in *P. polonicum* by incubation with FITC-labelled PgAFP. *P.*
291 *polonicum* showed green fluorescence only bound to the outer layer (Fig 5). However, the labelled protein
292 was found both inside the hyphae and bound to the outer layer in *A. tubingensis*, revealing that PgAFP
293 had entered *A. tubingensis*.

294 **Chitin-PgAFP binding assay**

295 Given that PgAFP was located at the outer layer of *P. polonicum*, a chitin-binding assay was performed.
296 When PgAFP was added to a solution of regenerated chitin, over 91% of the antifungal protein was
297 recovered from the supernatant after incubation, even at the lowest concentration tested (146 $\mu\text{g/ml}$).
298 Thus, PgAFP does not specifically bind to regenerated chitin.

299 **Effect on oxidative status and viability**

300 To test the influence of PgAFP on ROS production, staining with 2', 7' dichlorofluorescein diacetate was
301 used. Both treated and untreated *P. polonicum* showed similar levels of emitted fluorescence (data not
302 shown), revealing that PgAFP does not increase ROS in the resistant *P. polonicum*. The effect of PgAFP
303 on membrane integrity was evaluated by AO/EB double staining. EB was taken only by PgAFP-treated *A.*
304 *tubingensis*, showing orange hyphae, whilst non-treated *A. tubingensis* and both treated and non-treated *P.*
305 *polonicum* only showed green hyphae due to AO uptake (Fig. 6). These results reveal that *P. polonicum*
306 membrane was not compromised by PgAFP, which is the opposite to *A. tubingensis*. The evaluation of
307 apoptosis or necrosis confirmed the above reported effects on viability. *A. tubingensis* treated hyphae
308 showed orange color as a consequence of AnV-FITC and PI staining, meaning a necrotic stage. Non-
309 treated *A. tubingensis* and both treated and untreated *P. polonicum* were not dyed, showing no sign of
310 apoptosis or necrosis (Fig 7).

311 **DISCUSSION**

312 Both proteomic methods used in this work revealed differences in the relative abundance of proteins after
313 treatment of *P. polonicum* with PgAFP (Tables S1 and S2 in the Supplementary Material). Discrepancies

314 were detected in the fold change estimated by each method. Such discrepancies can be explained by the
315 fact that 2D-PAGE compares one isoform of a protein at a time, whereas label-free proteomics combines
316 every isoform together and gives the final total abundance of that protein (Delgado et al. 2015b).
317 Therefore, changes in the relative quantity of each isoform could be detected using 2D-PAGE, while in
318 the label-free proteomics only a measure of total abundance of all isoforms of a given protein is carried
319 out.
320 Label-free proteomics showed an increased abundance of 22 proteins related to ribosomes and
321 spliceosomes in PgAFP-treated *P. polonicum*, according to KEGG. However, only two ribosomal
322 proteins were found in higher amount by 2D-PAGE analysis. This fact can be explained by the narrow
323 range of pH chosen for 2D-PAGE analysis (Görg et al. 2009). In particular, the analysis carried out is
324 suitable for proteins with pI between 4-7, whilst proteins involved in ribosome structure or function are
325 generally out of this range (Görg et al. 2004). Therefore, the combinatorial deployment of proteomic tools
326 used in this study works complementarily to obtain further information about the effect of PgAFP on the
327 proteome.
328 The higher relative abundance of proteins from ribosomal and spliceosomal pathways in PgAFP-treated
329 *P. polonicum* could be regarded as a response of the mold to counteract the protein's antifungal activity. A
330 higher relative abundance of a substantial number of ribosomal and spliceosomal proteins has also been
331 described in a recent work on the effect of PgAFP on the sensitive *A. flavus* (Delgado et al. 2015b).
332 Twelve of the 22 proteins from this group that increased with PgAFP in *P. polonicum* also increased in *A.*
333 *flavus*. Thus, the increase in proteins from ribosomal and spliceosomal pathways solely would not explain
334 the resistance mechanism in *P. polonicum*.
335 The changes observed in the proteins related to metabolic pathways and biosynthesis of secondary
336 metabolites were heterogeneous, with 8 proteins increasing and 12 decreasing in PgAFP-treated *P.*
337 *polonicum* (Table 1). From these proteins, only pyruvate decarboxylase, aldehyde dehydrogenase, and
338 phosphatidylglycerol specific phospholipase showed similar changes in PgAFP-treated *A. flavus* (Delgado
339 et al. 2015b). However, these enzymes are scattered among various metabolic routes, including glycolysis
340 gluconeogenesis, purine metabolism, and aminoacyl-tRNA biosynthesis, making it unlikely that any of
341 them explain the ability of *P. polonicum* to withstand PgAFP.
342 All the above changes in the abundance of the metabolic-related proteins did not entail dramatic changes
343 in the metabolic activity, which in turn is consistent with the resistance of *P. polonicum* to PgAFP. The
344 abundance of intracellular red spots in FUN-1 staining (Fig. 2) revealed that the metabolic activity in *P.*
345 *polonicum* remained substantially unaffected by PgAFP, whereas it was greatly reduced in the sensitive
346 *A. tubingensis* used as a control (Fig 2), as well as in PgAFP-treated *A. flavus* (Delgado et al. 2015b).
347 Other effects reported for antifungal proteins, including PAF, NFAP, and PgAFP, are increased ROS
348 levels leading to programmed cell death in sensitive molds (Leiter et al. 2005; Galgóczy et al. 2013a;
349 Delgado et al. 2015b). Increased ROS levels have been linked to higher relative abundance of proteins
350 involved in the glutathione pathway and heat shock proteins in PgAFP-treated *A. flavus* (Delgado et al.
351 2015b). The limited changes in such stress-related proteins in treated *P. polonicum* do not reveal a strong
352 response to oxidative stress. In addition, none of the negative effects related to oxidative stress was

353 observed in PgAFP-treated *P. polonicum*, including increased ROS levels, loss of cell membrane
354 integrity, and necrotic signs.

355 All the changes in the proteome discussed so far reveal that PgAFP interacts with the non-sensitive *P.*
356 *polonicum*, but do not seem to explain the successful defence response. As discussed later, proteins from
357 the cell wall integrity (CWI) pathway seem to be involved in the successful defence response.

358 Membrane permeabilization is a main effect described for other antifungal proteins (Thevissen et al.
359 1999; Hagen et al. 2007). Increased permeability also contributes to PgAFP inhibition on *A. flavus*
360 (Delgado et al. 2015b). Similarly, the permeability of the sensitive *A. tubingensis* to SYTOX Green
361 increased at all PgAFP concentrations tested (Fig. 1). However, membrane permeabilization in *P.*
362 *polonicum* exhibited a two-step pattern: first increasing slowly at low PgAFP concentrations, then slowly
363 declining even below the level of untreated controls with the two highest concentrations tested (Fig. 1). A
364 similar two-step pattern in membrane permeabilization was also described for *Neurospora crassa* treated
365 with plant defensins (Thevissen et al. 1999). The lower permeability at the highest concentrations of
366 defensins has been explained by the apparent dependency of permeabilization on membrane polarization.
367 The higher permeability of fungal membranes treated with defensins causes depolarization, which may
368 ultimately decrease membrane permeability (Thevissen et al. 1996, 1999). The decline in *P. polonicum*
369 membrane permeability at high PgAFP concentrations might be partially explained by membrane
370 depolarization. As discussed later, other changes in membrane and cell wall can contribute to reach
371 permeability levels well below that in untreated controls.

372 Growth inhibition by AFP, PAF, and PgAFP has been related to the ability to interact with specific
373 molecules or anionic phospholipids in the cell wall and/or plasma membrane (Lacadena et al. 1998; Theis
374 et al. 2003; Marx et al. 2008; Delgado et al. 2015b). Similarly NFAP might bind to a G-protein coupled
375 receptor in a sensitive mold (Virágh et al. 2015) and AFP_{NN5353} does not bind to insensitive *Mucor*
376 *circinelloides* (Binder et al. 2011). Interestingly, PgAFP was located at the outer layer in the resistant *P.*
377 *polonicum* (Fig. 5). This binding may be due just to adherence to chitin or to specific receptors, but
378 PgAFP did not bind to regenerated chitin in vitro. Given that PgAFP was not internalized by the resistant
379 mold, no internal receptor can be detected. In addition, the proteome changes observed in PgAFP-treated
380 *P. polonicum* can only be due to transduction signals derived from the interaction with outer layer
381 receptors. Therefore, PgAFP may interact with specific molecules in the outer layer of *P. polonicum*,
382 similarly to PAF (Marx et al. 2008; Batta et al. 2009). As a consequence, PgAFP-resistance could be
383 related with the ability of *P. polonicum* to produce structural changes that prevent the interaction with the
384 specific receptors or the negatively charged phospholipids.

385 The fungal cell wall acts as an initial barrier in contact with hostile environments (Latgé 2007). The main
386 components of the cell wall that may act as a barrier against antifungal proteins are polysaccharides,
387 including glucans, glucomannans and chitin. A lower chitin content in the fungal cell wall has been
388 related to a higher permeability (Mellado et al. 2003; Rementeria et al. 2005), suggesting a barrier role of
389 chitin. The higher amount of chitin observed in the cell wall of *P. polonicum* treated with the highest
390 PgAFP concentration (Fig. 3) can be responsible for the lower permeability observed, being a key factor
391 in the successful response to this antifungal protein. Chitin synthesis is also stimulated by AFP in
392 resistant fungi (Ouedraogo et al. 2011), but not by AFP, PAF, and PgAFP in sensitive molds (Hagen et al.

2007; Binder et al. 2010; Delgado et al. 2015b). In addition, PAF and NFAP provoke delocalized chitin deposition at the hyphal tips (Binder et al. 2010; Virágh et al. 2015). Therefore, the altered chitin deposition can be related to sensitivity to antifungal proteins in contrast to our findings in *P. polonicum*.

To confirm if the increased chitin deposition itself is enough to explain the resistance to PgAFP, a joint treatment of PgAFP and chitinase was applied to *P. polonicum*. The slowest growth obtained with the combined treatment strongly infers that the increased chitin content plays a key role in the resistance of *P. polonicum* to PgAFP. Therefore, we propose that chitin cell wall reinforcement is responsible for the successful response of *P. polonicum*, due to a hampered interaction of PgAFP with specific receptors or the negatively charged phospholipids.

From the proteins involved in chitin biosynthesis, glucosamine-6-phosphate N-acetyl transferase was only found in treated *P. polonicum* (Table 1). The gene coding for this protein, as well as the gene encoding an α -1,3-glucan synthase, is upregulated in *A. niger* treated with sublethal doses of caspofungin (Meyer et al. 2007). Given that an increase of glucan but not chitin synthesis results in an ineffective survival response (Hagen et al. 2007), the increase in glucosamine-6-phosphate N-acetyl transferase could be important for *P. polonicum* to counteract PgAFP. The increased chitin content can also be related with CWI signaling activation. The stress signals sensed by the receptor protein Wsc are transmitted to Rho1, which has been considered the master regulator of cell wall integrity signaling pathway in yeasts (Levin 2005). Then, Rho1 binds and activates Pkc (Nonaka et al. 1995; Kamada et al. 1996; Lodder et al. 1999), and the signals channeled through the Mpk signaling lead to activation of genes involved in cell wall synthesis (Igual et al. 1996; Jung and Levin 1999), resulting in an elevated chitin content (Munro et al. 2007). Rho1 and Pkc1 have been suggested as the only proteins of CWI pathway that could be involved in the survival response of AFP-resistant *Saccharomyces cerevisiae*, but its relevance has not been established (Ouedraogo et al. 2011).

In sensitive molds, chitin synthesis is not increased by antifungal proteins, as for *A. nidulans* treated with PAF (Binder et al. 2010) or *A. niger* treated with AFP (Hagen et al. 2007). The resistant *P. polonicum* showed an increased abundance of Rho1 and in chitin synthesis when treated with PgAFP (Table 1 and Fig. 3). Conversely, the sensitive *A. flavus* showed a lower relative abundance of Rho1 and a lower chitin deposition when treated with PgAFP (Delgado et al. 2015b). Therefore, it seems that the efficient response of CWI pathway activation by Rho1 could be a key role in the resistance to PgAFP, in contrast to the basal ineffective compensatory response of this pathway in sensitive molds.

In conclusion, the proteome changes and the altered permeability imply an active reaction of *P. polonicum* to PgAFP, where the increased chitin content can be related with a higher abundance of glucosamine-6-phosphate N-acetyltransferase and Rho1. Moreover, the combined treatment with chitinase could provide a complementary means to combat resistance to antifungal proteins.

ACKNOWLEDGEMENTS

This work was supported by the Spanish Ministry of Education and Science, Ministry of Economy and Competitiveness and FEDER (AGL2010-21623, AGL2013-45729-P). Josué Delgado was recipient of a FPI grant from the Spanish Ministry of Education and Science (BES-2011-043422 y EEBB-I-13-06900). Rebecca A. Owens was funded by a 3U Partnership Award (<http://www.3UPartnership.ie/>). Mass

432 spectrometry facilities were funded by Science Foundation Ireland (Q-Exactive; 12/RI/2346(3) &
433 PI/11/1188) and the Irish Higher Education Authority (Agilent Ion Trap 6340).

434 **ETHICAL STATEMENT**

435 This article does not contain any studies with human participants or animals performed by any of the
436 authors.

437 **CONFLICT OF INTEREST**

438 The authors declare that they have no conflict of interest.

439 **BIBLIOGRAPHY**

- 440 Acosta R, Rodríguez-Martín A, Martín A, Núñez F, Asensio MA (2009) Selection of antifungal protein-
441 producing molds from dry-cured meat products. *Int J Food Microbiol* 135:39–46. doi:
442 10.1016/j.ijfoodmicro.2009.07.020
- 443 Batta G, Barna T, Gáspári Z, Sándor S, Kövér KE, Binder U, Sarg B, Kaiserer L, Chhillar AK, Eigentler
444 A, Leiter E, Hegedüs N, Pócsi I, Lindner H, Marx F (2009) Functional aspects of the solution
445 structure and dynamics of PAF-a highly-stable antifungal protein from *Penicillium chrysogenum*.
446 *FEBS J* 276:2875–2890. doi: 10.1111/j.1742-4658.2009.07011.x
- 447 Binder U, Oberparleiter C, Meyer V, Marx F (2010) The antifungal protein PAF interferes with
448 PKC/MPK and cAMP/PKA signalling of *Aspergillus nidulans*. *Mol Microbiol* 75:294–307. doi:
449 10.1111/j.1365-2958.2009.06936.x
- 450 Binder U, Bencina M, Eigentler A, Meyer V, Marx F (2011) The *Aspergillus giganteus* antifungal protein
451 AFPNN5353 activates the cell wall integrity pathway and perturbs calcium homeostasis. *BMC*
452 *Microbiol* 11:209. doi: 10.1186/1471-2180-11-209
- 453 Binder U, Benčina M, Fizil Á, Batta G, Chhillar AK, Marx F (2015) Protein kinase A signaling and
454 calcium ions are major players in PAF mediated toxicity against *Aspergillus niger*. *FEBS Lett*
455 589:1266–1271. doi: 10.1016/j.febslet.2015.03.037
- 456 Carberry S, Neville CM, Kavanagh KA, Doyle S (2006) Analysis of major intracellular proteins of
457 *Aspergillus fumigatus* by MALDI mass spectrometry: identification and characterisation of an
458 elongation factor 1B protein with glutathione transferase activity. *Biochem Biophys Res Commun*
459 341:1096–1104. doi: 10.1016/j.bbrc.2006.01.078
- 460 Carpentier SC, Witters E, Laukens K, Deckers P, Swennen R, Panis B (2005) Preparation of protein
461 extracts from recalcitrant plant tissues: an evaluation of different methods for two-dimensional gel
462 electrophoresis analysis. *Proteomics* 5:2497–2507. doi: 10.1002/pmic.200401222
- 463 Chen Z, Ao J, Yang W, Jiao L, Zheng T, Chen X (2013) Purification and characterization of a novel
464 antifungal protein secreted by *Penicillium chrysogenum* from an Arctic sediment. *Appl Microbiol*
465 *Biotechnol* 97:10381–10390. doi: 10.1007/s00253-013-4800-6
- 466 Collins C, Keane TM, Turner DJ, O’Keeffe G, Fitzpatrick DA, Doyle S (2013) Genomic and proteomic
467 dissection of the ubiquitous plant pathogen, *Armillaria mellea*: Toward a new infection model
468 system. *J Proteome Res* 12:2552–2570. doi: 10.1021/pr301131t
- 469 Conesa A, Götz S, García-Gómez JM, Terol J, Talón M, Robles M (2005) Blast2GO: A universal tool for
470 annotation, visualization and analysis in functional genomics research. *Bioinformatics* 21:3674–
471 3676. doi: 10.1093/bioinformatics/bti610

472 Cox J, Mann M (2008) MaxQuant enables high peptide identification rates, individualized p.p.b.-range
473 mass accuracies and proteome-wide protein quantification. *Nat Biotechnol* 26:1367–1372. doi:
474 10.1038/nbt.1511

475 Delgado J, Acosta R, Rodríguez-Martín A, Bermúdez E, Núñez F, Asensio MA (2015a) Growth
476 inhibition and stability of PgAFP from *Penicillium chrysogenum* against fungi common on dry-
477 ripened meat products. *Int J Food Microbiol* 205:23–29. doi: 10.1016/j.ijfoodmicro.2015.03.029

478 Delgado J, Owens RA, Doyle S, Asensio MA, Núñez F (2015b) Impact of the antifungal protein PgAFP
479 from *Penicillium chrysogenum* on the protein profile in *Aspergillus flavus*. *Appl Microbiol*
480 *Biotechnol* In press doi: 10.1007/s00253-015-6731-x

481 Dolan SK, Owens RA, O’Keeffe G, Hammel S, Fitzpatrick DA, Jones GW, Doyle S (2014) Regulation of
482 nonribosomal peptide synthesis: bis-thiomethylation attenuates gliotoxin biosynthesis in *Aspergillus*
483 *fumigatus*. *Chem Biol* 21:999–1012. doi: 10.1016/j.chembiol.2014.07.006

484 Galgóczy L, Kovács L, Karácsony Z, Virágh M, Hamari Z, Vágvölgyi C (2013a) Investigation of the
485 antimicrobial effect of *Neosartorya fischeri* antifungal protein (NFAP) after heterologous
486 expression in *Aspergillus nidulans*. *Microbiology* 159:411–419. doi: 10.1099/mic.0.061119-0

487 Galgóczy L, Virágh M, Kovács L, Tóth B, Papp T, Vágvölgyi C (2013b) Antifungal peptides
488 homologous to the *Penicillium chrysogenum* antifungal protein (PAF) are widespread among
489 *Fusaria*. *Peptides* 39:131–137. doi: 10.1016/j.peptides.2012.10.016

490 Görg A, Weiss W, Dunn MJ (2004) Current two-dimensional electrophoresis technology for proteomics.
491 *Proteomics* 4:3665–3685. doi: 10.1002/pmic.200401031

492 Görg A, Drews O, Lück C, Weiland F, Weiss W (2009) 2-DE with IPGs. *Electrophoresis* 30 Suppl
493 1:S122–S132. doi: 10.1002/elps.200900051

494 Gun Lee D, Shin SY, Maeng CY, Jin ZZ, Kim KL, Hahm KS (1999) Isolation and characterization of a
495 novel antifungal peptide from *Aspergillus niger*. *Biochem Biophys Res Commun* 263:646–651. doi:
496 10.1006/bbrc.1999.1428

497 Hagen S, Marx F, Ram AF, Meyer V (2007) The antifungal protein AFP from *Aspergillus giganteus*
498 inhibits chitin synthesis in sensitive fungi. *Appl Environ Microbiol* 73:2128–2134. doi:
499 10.1128/AEM.02497-06

500 Hajji M, Jellouli K, Hmidet N, Balti R, Sellami-Kamoun A, Nasri M (2010) A highly thermostable
501 antimicrobial peptide from *Aspergillus clavatus* ES1: Biochemical and molecular characterization. *J*
502 *Ind Microbiol Biotechnol* 37:805–813. doi: 10.1007/s10295-010-0725-6

503 Harris SD, Morrell JL, Hamer JE (1994) Identification and characterization of *Aspergillus nidulans*
504 mutants defective in cytokinesis. *Genetics* 136:517–532

505 Houbraeken J, Samson RA (2011) Phylogeny of *Penicillium* and the segregation of *Trichocomaceae* into
506 three families. *Stud Mycol* 70:1–51. doi: 10.3114/sim.2011.70.01

507 Igual JC, Johnson a L, Johnston LH (1996) Coordinated regulation of gene expression by the cell cycle
508 transcription factor Swi4 and the protein kinase C MAP kinase pathway for yeast cell integrity.
509 *EMBO J* 15:5001–5013

510 Jung US, Levin DE (1999) Genome-wide analysis of gene expression regulated by the yeast cell wall
511 integrity signalling pathway. *Mol Microbiol* 34:1049–1057

512 Kaiserer L, Oberparleiter C, Weiler-Görz R, Burgstaller W, Leiter E, Marx F (2003) Characterization of
513 the *Penicillium chrysogenum* antifungal protein PAF. *Arch Microbiol* 180:204–210. doi:
514 10.1007/s00203-003-0578-8

515 Kamada Y, Qadota H, Python CP, Anraku Y, Ohya Y, Levin DE (1996) Activation of yeast protein
516 kinase C by Rho1 GTPase. *J Biol Chem* 271:9193–9196. doi: 10.1074/jbc.271.16.9193

1 517 Kim Y, Nandakumar MP, Marten MR (2007) Proteomics of filamentous fungi. Trends Biotechnol
2 518 25:395–400. doi: 10.1016/j.tibtech.2007.07.008

3 519 Kovács L, Virágh M, Takó M, Papp T, Vágvölgyi C, Galgóczy L (2011) Isolation and characterization of
4 520 *Neosartorya fischeri* antifungal protein (NFAP). Peptides 32:1724–1731. doi:
5 521 10.1016/j.peptides.2011.06.022

6 522 Lacadena J, Martínez del Pozo A, Lacadena V, Martínez-Ruiz A, Mancheño JM, Oñaderra M, Gavilanes
7 523 JG (1998) The cytotoxin α -sarcin behaves as a cyclizing ribonuclease. FEBS Lett 424:46–48. doi:
8 524 10.1016/S0014-5793(98)00137-9

9 525 Latgé J-P (2007) The cell wall: a carbohydrate armour for the fungal cell. Mol Microbiol 66:279–290.
10 526 doi: 10.1111/j.1365-2958.2007.05872.x

11 527 Leiter É, Szappanos H, Oberparleiter C, Kaiserer L, Csernoch L, Pusztahelyi T, Emri T, Pócsi I,
12 528 Salvenmoser W, Marx F (2005) Antifungal protein PAF severely affects the integrity of the plasma
13 529 membrane of *Aspergillus nidulans* and induces an apoptosis-like phenotype. Antimicrob Agents
14 530 Chemother 49:2445–2453. doi: 10.1128/AAC.49.6.2445

15 531 Levin DE (2005) Cell wall integrity signaling in *Saccharomyces cerevisiae*. Microbiol Mol Biol Rev
16 532 69:262–291. doi: 10.1128/MMBR.69.2.262

17 533 Liu R, Huang H, Yang Q, Liu W-Y (2002) Purification of α -sarcin and an antifungal protein from mold
18 534 (*Aspergillus giganteus*) by chitin affinity chromatography. Protein Expr Purif 25:50–58. doi:
19 535 10.1006/prep.2001.1608

20 536 Lodder AL, Lee TK, Ballester R (1999) Characterization of the Wsc1 protein, a putative receptor in the
21 537 stress response of *Saccharomyces cerevisiae*. Genetics 152:1487–1499

22 538 Lowry OH, Rosebrough NJ, Farr L, Randall RJ (1951) Protein measurement with the Folin phenol
23 539 reagent. J Biol Chem 193:265–275

24 540 Marx F, Haas H, Reindl M, Stöffler G, Lottspeich F, Redl B (1995) Cloning, structural organization and
25 541 regulation of expression of the *Penicillium chrysogenum paf* gene encoding an abundantly secreted
26 542 protein with antifungal activity. Gene 167:167–171

27 543 Marx F, Binder U, Leiter E, Pócsi I (2008) The *Penicillium chrysogenum* antifungal protein PAF, a
28 544 promising tool for the development of new antifungal therapies and fungal cell biology studies. Cell
29 545 Mol Life Sci 65:445–454. doi: 10.1007/s00018-007-7364-8

30 546 Mellado E, Dubreucq G, Mol P, Sarfati J, Paris S, Diaquin M, Holden DW, Rodriguez-Tudela JL, Latgé
31 547 JP (2003) Cell wall biogenesis in a double chitin synthase mutant (*chsG*-/*chsE*-) of *Aspergillus*
32 548 *fumigatus*. Fungal Genet Biol 38:98–109. doi: 10.1016/S1087-1845(02)00516-9

33 549 Meyer V, Damveld RA, Arentshorst M, Stahl U, Van Den Hondel C, Ram A (2007) Survival in the
34 550 presence of antifungals: Genome-wide expression profiling of *Aspergillus niger* in response to
35 551 sublethal concentrations of caspofungin and fenpropimorph. J Biol Chem 282:32935–32948. doi:
36 552 10.1074/jbc.M705856200

37 553 Moreno AB, Del Pozo AM, Borja M, Segundo BS (2003) Activity of the antifungal protein from
38 554 *Aspergillus giganteus* against *Botrytis cinerea*. Phytopathology 93:1344–1353. doi:
39 555 10.1094/PHYTO.2003.93.11.1344

40 556 Moreno AB, Martínez Del Pozo Á, San Segundo B (2006) Antifungal mechanism of the *Aspergillus*
41 557 *giganteus* AFP against the rice blast fungus *Magnaporthe grisea*. Appl Microbiol Biotechnol
42 558 72:883–895. doi: 10.1007/s00253-006-0362-1

43 559 Munro CA, Selvaggini S, De Bruijn I, Walker L, Lenardon MD, Gerssen B, Milne S, Brown AJP, Gow
44 560 NAR (2007) The PKC, HOG and Ca^{2+} signalling pathways co-ordinately regulate chitin synthesis
45 561 in *Candida albicans*. Mol Microbiol 63:1399–1413. doi: 10.1111/j.1365-2958.2007.05588.x

562 Nakaya K, Omata K, Okahashi I, Nakamura Y, Kolkenbrock H, Ulbrich N (1990) Amino acid sequence
1 563 and disulfide bridges of an antifungal protein isolated from *Aspergillus giganteus*. Eur J Biochem
2 564 193:31–38

3
4 565 Nonaka H, Tanaka K, Hirano H, Fujiwara T, Kohno H, Umikawa M, Mino A, Takai Y (1995) A
5 566 downstream target of RHO1 small GTP-binding protein is PKC1, a homolog of protein kinase C,
6 567 which leads to activation of the MAP kinase cascade in *Saccharomyces cerevisiae*. EMBO J
7 568 14:5931–5938

8
9 569 O’Keeffe G, Jöchl C, Kavanagh K, Doyle S (2013) Extensive proteomic remodeling is induced by
10 570 eukaryotic translation elongation factor 1B γ deletion in *Aspergillus fumigatus*. Protein Sci 22:1612–
11 571 1622. doi: 10.1002/pro.2367

12
13 572 O’Keeffe G, Hammel S, Owens RA, Keane TM, Fitzpatrick DA, Jones GW, Doyle S (2014) RNA-seq
14 573 reveals the pan-transcriptomic impact of attenuating the gliotoxin self-protection mechanism in
15 574 *Aspergillus fumigatus* BMC Genomics. 25:1–26. doi: 10.1186/1471-2164-15-894

16
17 575 Ouedraogo JP, Hagen S, Spielvogel A, Engelhardt S, Meyer V (2011) Survival strategies of yeast and
18 576 filamentous fungi against the antifungal protein AFP. J Biol Chem 286:13859–13868. doi:
19 577 10.1074/jbc.M110.203588

20
21 578 Owens RA, Hammel S, Sheridan KJ, Jones GW, Doyle S (2014) A proteomic approach to investigating
22 579 gene cluster expression and secondary metabolite functionality in *Aspergillus fumigatus*. PLoS
23 580 ONE 9:e106942

24
25 581 Rementeria A, López-Molina N, Ludwig A, Vivanco AB, Bikandi J, Pontón J, Garaizar J (2005) Genes
26 582 and molecules involved in *Aspergillus fumigatus* virulence. Rev Iberoam Micol 22:1–23. doi:
27 583 2005221

28
29 584 Rodríguez-Martín A, Acosta R, Liddell S, Núñez F, Benito MJ, Asensio MA (2010) Characterization of
30 585 the novel antifungal protein PgAFP and the encoding gene of *Penicillium chrysogenum*. Peptides
31 586 31:541–547. doi: 10.1016/j.peptides.2009.11.002

32
33 587 Seibold M, Wolschann P, Bodevin S, Olsen O (2011) Properties of the bubble protein, a defensin and an
34 588 abundant component of a fungal exudate. Peptides 32:1989–1995. doi:
35 589 10.1016/j.peptides.2011.08.022

36
37 590 Shevchenko A, Tomas H, Havlis J, Olsen J V, Mann M (2007) In-gel digestion for mass spectrometric
38 591 characterization of proteins and proteomes. Nat Protoc 1:2856–2860. doi: 10.1038/nprot.2006.468

39
40 592 Skouri-Gargouri H, Gargouri A (2008) First isolation of a novel thermostable antifungal peptide secreted
41 593 by *Aspergillus clavatus*. Peptides 29:1871–1877. doi: 10.1016/j.peptides.2008.07.005

42
43 594 Skouri-Gargouri H, Ali MB, Gargouri A (2009) Molecular cloning, structural analysis and modelling of
44 595 the antifungal peptide from *Aspergillus clavatus*. Peptides 30:1798–1804.
45 596 10.1016/j.peptides.2009.06.034

46
47 597 Souza CP, Burbano-Rosero EM, Almeida BC, Martins GG, Albertini LS, Rivera ING (2009) Culture
48 598 medium for isolating chitinolytic bacteria from seawater and plankton. World J Microbiol
49 599 Biotechnol 25:2079–2082. doi: 10.1007/s11274-009-0098-z

50
51 600 Theis T, Wedde M, Meyer V, Stahl U (2003) The antifungal protein from *Aspergillus giganteus* causes
52 601 membrane permeabilization. Antimicrob Agents Chemother 47:588–593. doi:
53 602 10.1128/AAC.47.2.588

54
55 603 Thevissen K, Ghazi A, De Samblanx GW, Brownlee C, Osborn RW, Broekaert WF (1996) Fungal
56 604 membrane responses induced by plant defensins and thionins. J Biol Chem 271:15018–15025

57
58 605 Thevissen K, Terras FR, Broekaert WF (1999) Permeabilization of fungal membranes by plant defensins
59 606 inhibits fungal growth. Appl Environ Microbiol 65:5451–5458

607 Virágh, M., Marton, A., Vizler, C., Tóth, L., Vágvölgyi, C., Marx, F., Galgóczy, L., 2015. Insight into the
608 antifungal mechanism of *Neosartorya fischeri* antifungal protein. *Protein Cell* 6, 518–528.
609 doi:10.1007/s13238-015-0167-z

610 Yeaman MR, Yount NY (2003) Mechanisms of antimicrobial peptide action and resistance. *Pharmacol*
611 *Rev* 55:27–55. doi: 10.1124/pr.55.1.2

612 FIGURE CAPTIONS

613 **Fig. 1** SYTOX Green uptake with different concentrations of PgAFP on *P. polonicum* and *A. tubingensis*
614 at 24 h (bars represent standard deviation of the mean).

615
616 **Fig.2** Metabolic activity of *P. polonicum* (panel A) and *A. tubingensis* (panel B) tested with FUN-1
617 staining. Non-treated hyphae (left) showed intravacuolar activity as red spots. Hyphae treated with 75
618 $\mu\text{g/ml}$ PgAFP for 24 h (right) showed intravacuolar activity in *P. polonicum*, but very low metabolic
619 activity in *A. tubingensis*.

620
621 **Fig. 3** Chitin distribution on *P. polonicum* stained with fluorescent brightener 28. Left: non-treated
622 hyphae; right: hyphae treated with 75 $\mu\text{g/ml}$ PgAFP for 24 h.

623
624 **Fig. 4** Effect of PgAFP and chitinase combined treatment on *P. polonicum* growth. Untreated control:
625 added with 2.5 ml of phosphate elution buffer and 100 μl PBS; PgAFP: added with 2.5 ml of 600 $\mu\text{g/ml}$
626 PgAFP in phosphate elution buffer and 100 μl PBS. Chitinase: added with 2.5 ml of phosphate elution
627 buffer and 100 μl of ≥ 60 units/ml chitinase from *Streptomyces griseus*; PgAFP + Chitinase: added with
628 2.5 ml of 600 $\mu\text{g/ml}$ PgAFP in phosphate elution buffer and 100 μl PBS.

629
630 **Fig. 5** PgAFP localization in *P. polonicum* (left) and *A. tubingensis* (right) treated with 20 $\mu\text{g/ml}$ FITC-
631 labelled PgAFP for 24 h. PgAFP was found solely bound to the outer layer in *P. polonicum* but mainly
632 inside *A. tubingensis*.

633
634 **Fig. 6** Effect of 75 $\mu\text{g/ml}$ PgAFP on membrane integrity of *P. polonicum* (left) and *A. tubingensis* (right)
635 evaluated with vital acridine orange (AO) / ethidium bromide (EB) staining. *P. polonicum* hyphae showed
636 intense green color due to only AO penetration through non-compromised membrane. *A. tubingensis*
637 hyphae showed intense orange color due to both AO and EB penetration through compromised cell
638 membrane.

639
640 **Fig. 7** Effect of 75 $\mu\text{g/ml}$ PgAFP on *P. polonicum* and *A. tubingensis* hyphae viability evaluated with
641 apoptosis detection kit at 24 h of incubation. A: Non-treated *P. polonicum*. B: PgAFP-treated *P.*
642 *polonicum*. C: Non-treated *A. tubingensis*. D: PgAFP-treated *A. tubingensis*. Left: Annexin V/FITC-
643 Propidium Iodide (An/FITC-PI) staining. Right: The corresponding bright field view. No intense green or
644 orange color due to apoptosis or necrosis was observed in PgAFP-treated *P. polonicum*. Only PgAFP-
645 treated *A. tubingensis* showed intense orange color due to necrosis.

Table 1. Selected proteins whose relative abundance was affected by PgAFP in *Penicillium polonicum* reaching over 2.0 fold change in Label-Free Proteomics (LFP) analysis or 1.5 fold change in 2D-PAGE. Data are given according to four groups of metabolic pathways.

Proteins involved in pathways	Fold change	Detection method
Ribosomal and spliceosomal proteins		
Pc12g05940 40s ribosomal protein s13	T ^a	LFP
Pc13g01870 60s ribosomal protein l16	T	LFP
Pc16g04770 formin binding protein	T	LFP
Pc20g10480 small nuclear ribonucleoprotein	T	LFP
Pc22g08360 pre-mrna branch site protein p14	T	LFP
Pc20g00680 60s ribosomal protein l23	+11.16	LFP
Pc20g13260 ribosomal protein l14	+6.32	LFP
Pc13g02890 60s ribosomal protein l27	+5.32	LFP
Pc13g05540 60s ribosomal protein l18	+4.17	LFP
Pc18g04110 60s ribosomal protein l34	+4.05	LFP
Pc22g02060 60s ribosomal protein l8	+3.88	LFP
Pc21g16520 60s ribosomal protein l4	+3.83	LFP
Pc16g14740 40s ribosomal protein s22	+3.21	LFP
Pc16g09160 60s ribosomal protein l15	+3.14	LFP
Pc22g00880 40s ribosomal protein s18	+2.73	LFP
Pc21g18200 60s ribosomal protein	+2.51	LFP
Pc16g12990 60s ribosomal protein l17	+2.47	LFP
Pc13g07190 60s ribosomal protein l11	+2.32	LFP
Pc13g05920 60s ribosomal protein l7	+2.21	LFP
Pc20g03340 60s ribosomal protein l33	+2.19	LFP
Pc13g06740 60s ribosomal protein l13	+2.06	LFP
Pc20g02900 40s ribosomal protein s4	+2.02	LFP
Biosynthesis of secondary metabolites and metabolic pathway		
Pc21g21940 bifunctional pyrimidine biosynthesis protein	T	LFP
Pc22g06070 glycerol kinase	T	LFP
Pc22g17940 asparagine synthetase	T	LFP
Pc22g23800 glucosamine 6-phosphate N-acetyl transferase ^b	T	LFP
Pc21g15760 glutamyl-trna synthetase	+12.44	LFP
Pc20g07710 sulfate adenylyltransferase	+6.9	LFP
Pc22g07020 nitrilase	+3.49	LFP
Pc18g01490 pyruvate decarboxylase	+2.01	LFP
Phosphoglucomutase	-2	2D-PAGE
Pc16g05080 adenosylhomocysteinase	-2	LFP
Pc12g05750 d-xylulose kinase	-2.31	LFP
Pc21g04710 phospho-2-dehydro-3-deoxyheptonate aldolase	-2.52	LFP
Pc22g19440 aspartate aminotransferase	-2.58	LFP
Pc21g03190 glycerate dehydrogenase	-2.66	LFP
Pc22g02810 methylmalonate-semialdehyde dehydrogenase	-3.05	LFP
Pc22g19730 glucose-6-phosphate isomerase	-3.49	LFP
Pc15g01900 putative oligo-glucosidase	-6.9	LFP
Pc15g01880 phosphatidylglycerol specific phospholipase	-633	LFP
Pc13g03600 thiamine biosynthetic bifunctional	NT ^c	LFP
Pc14g00170 phosphatidylglycerol specific	NT	LFP
Pc22g24860 aldehyde dehydrogenase	NT	LFP
CWI pathway		
Pc22g23800 glucosamine-6-phosphate N-acetyl transferase ^b	NT	LFP
Pc14g01930 protein Rho gtpase rho1	+9.04	LFP
Pc21g11950 UDP-N-acetylglucosamine pyrophosphorylase	-2	2D-PAGE
UDP-glucose 4-epimerase	-1.5	2D-PAGE
Gamma-actin act	-1.6	2D-PAGE

^a T: Protein only detected in treated samples.

^b Protein involved in more than one pathway.

^c NT: Protein only detected in non-treated samples.

Figure 1

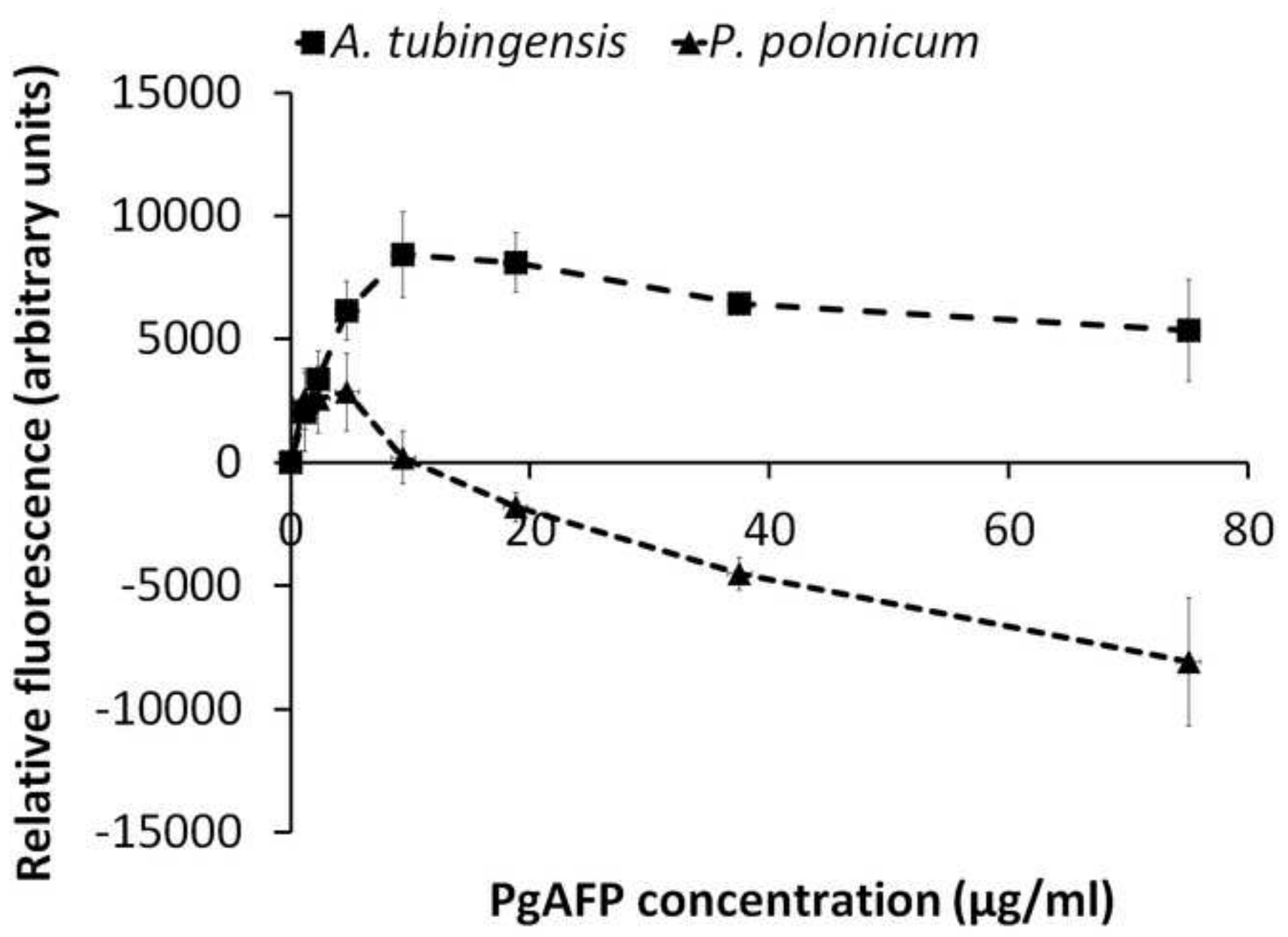


Figure2

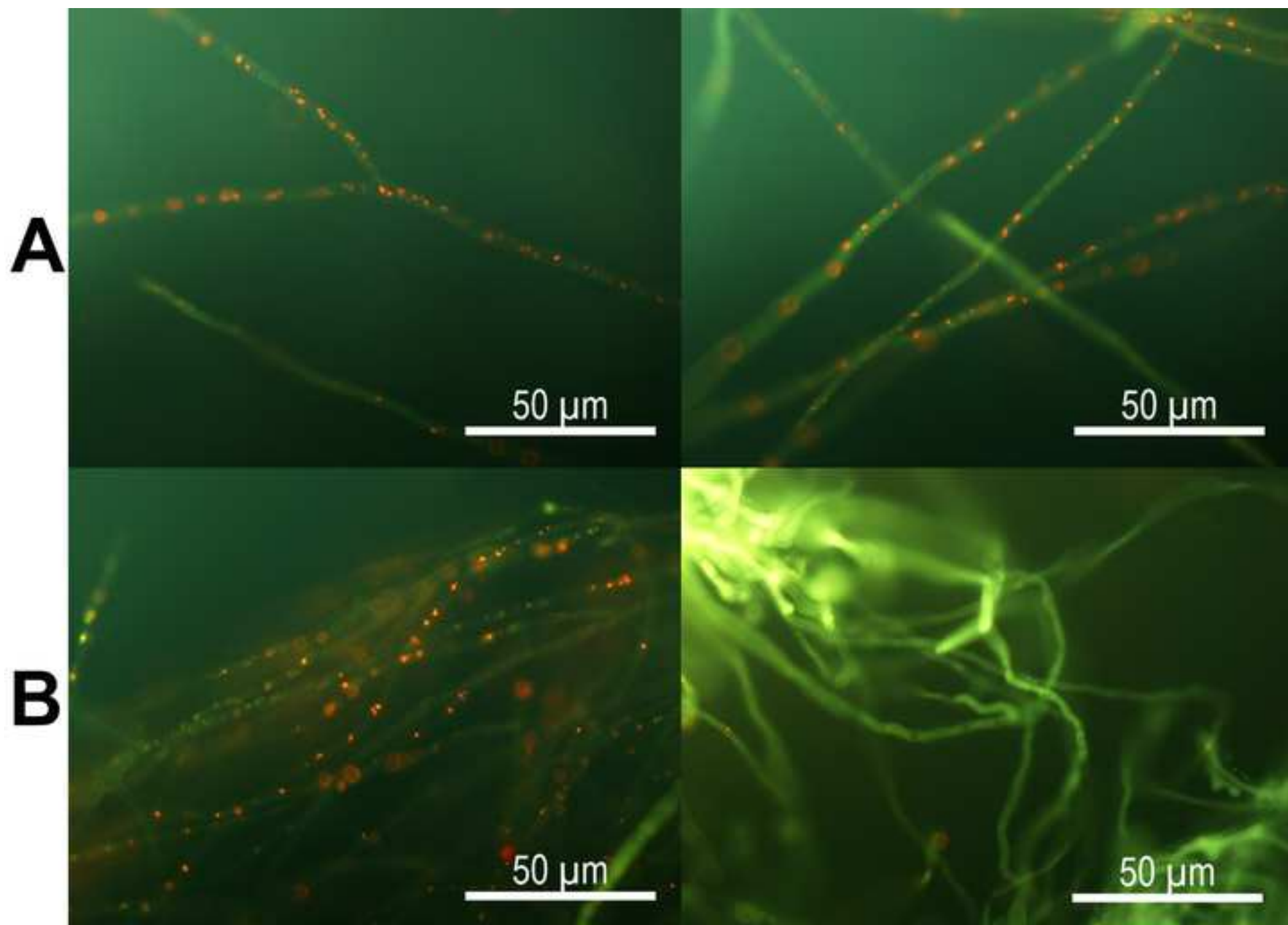


Figure 3

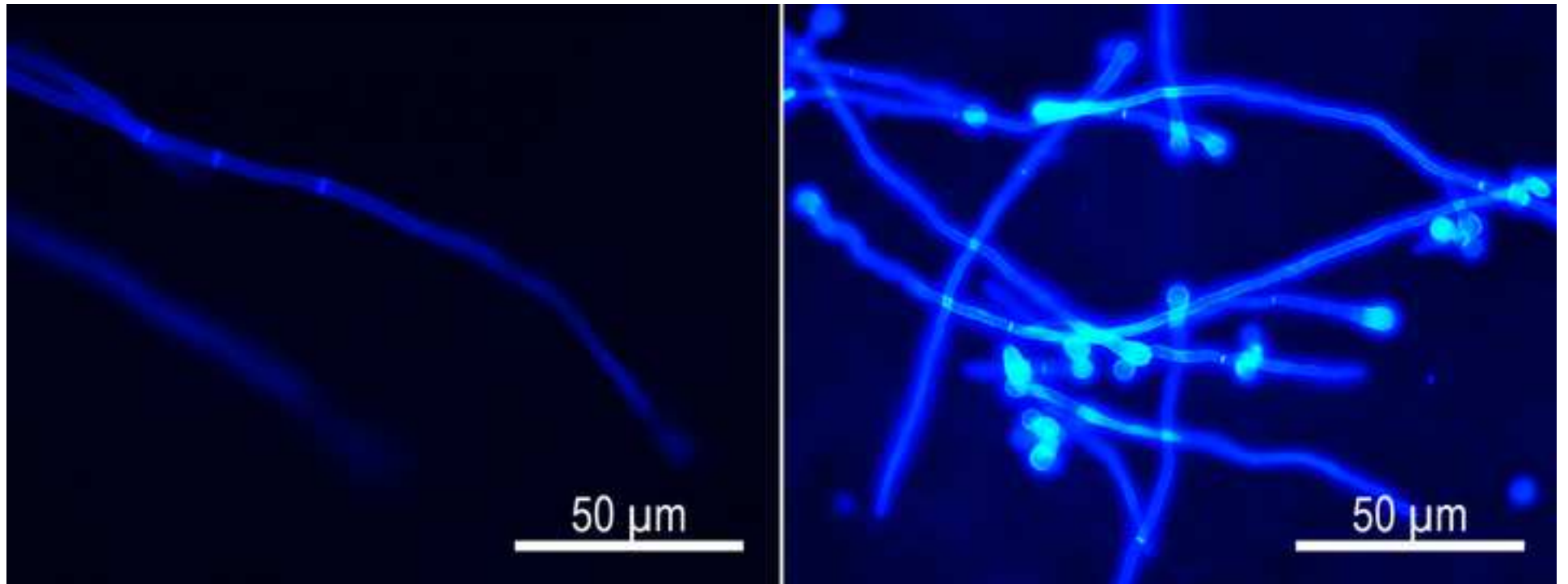


Figure 4

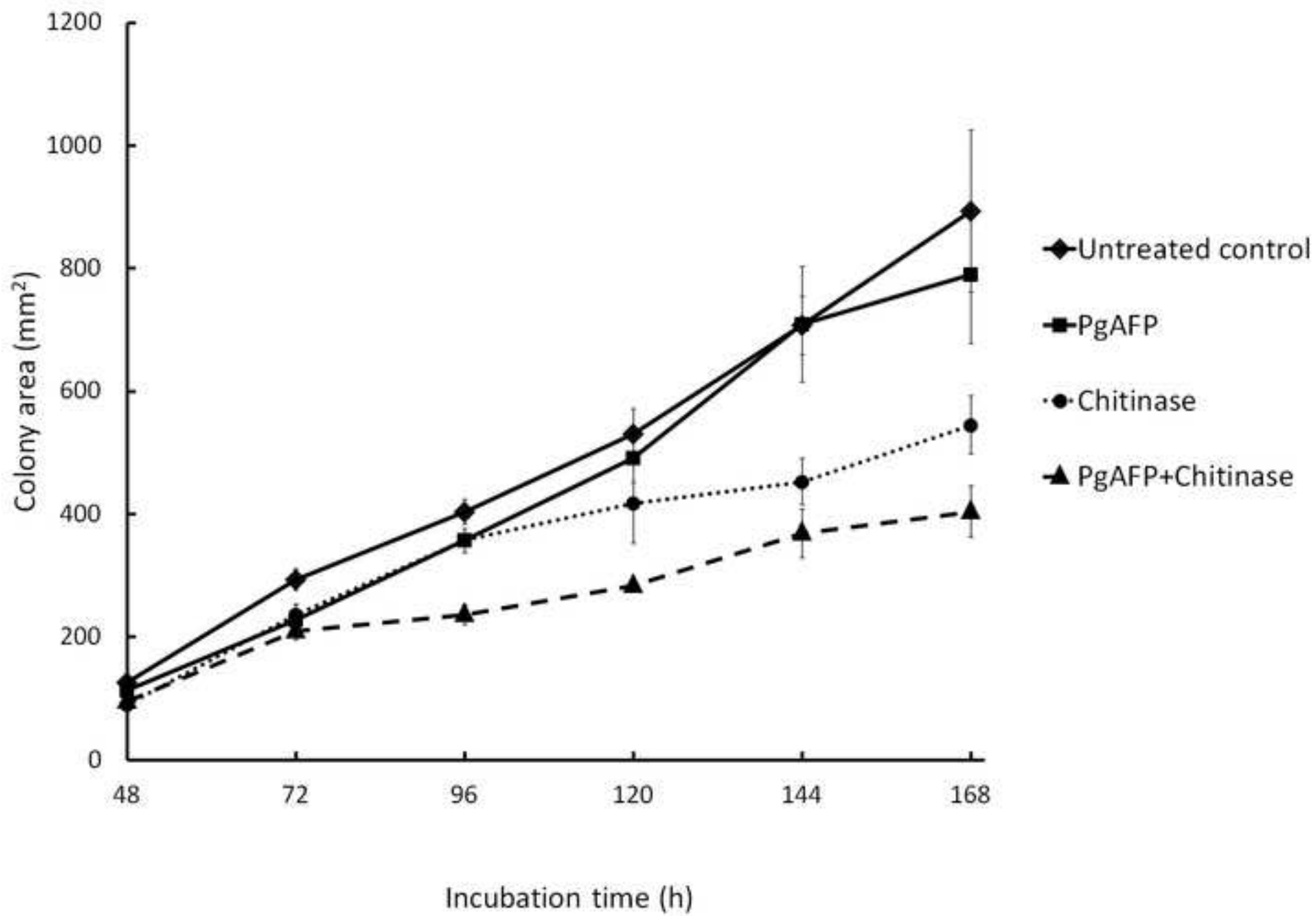


Figure 5

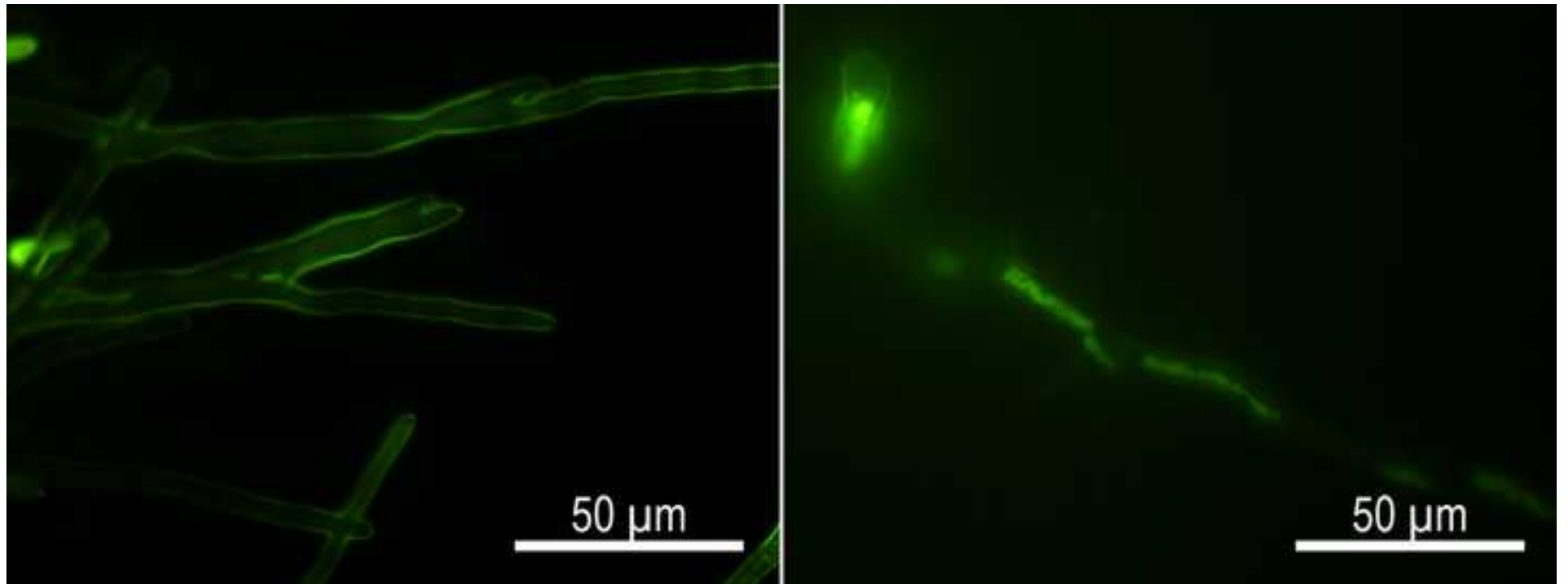


Figure 6

